Nuclear Bile Acid Receptor FXR Protects against Intestinal Tumorigenesis

Salvatore Modica,[1] Stefania Murzilli,[1] Lorena Salvatore,[1] Daniel R. Schmidt,[2] and Antonio Moschetta[1]

[1]Laboratory of Lipid Metabolism and Cancer, Department of Translational Pharmacology, Consorzio Mario Negri Sud, Santa Maria Imbaro, Chieti and Clinica Medica "A. Murri," University of Bari, Bari, Italy and [2]Department of Pharmacology, University of Texas Southwestern Medical Center, Dallas, Texas

Abstract

Bile acids have been considered intestinal tumor promoters, and because they are natural ligands for the nuclear receptor FXR, we examined the role of FXR in intestinal tumorigenesis. Using gain- and loss-of-function studies, we found that FXR suppresses intestinal tumorigenesis *in vivo*. Loss of FXR in the $Apc^{Min/+}$ and in the chronic colitis mouse models of intestinal tumorigenesis resulted in early mortality and increased tumor progression via promotion of Wnt signaling by infiltrating neutrophils and macrophages and tumor necrosis factor α production. Treatment with the bile acid binding resin cholestyramine did not modify the intestinal tumor susceptibility of $FXR^{-/-}$ mice, indicating that loss of FXR and not merely elevated bile acid concentrations increases susceptibility to tumorigenesis. Activation of FXR induced a proapoptotic program in the differentiated normal colonic epithelium as well as transformed colonocytes. Our data suggest that it is unlikely that the tumor-promoting activity of bile acids occurs as a function of their ability to activate FXR. However, FXR activity is relevant to the pathogenesis of intestinal cancer. When FXR is absent in the intestine, there is a promotion of Wnt signaling with expansion of the basal proliferative compartment, and a concomitant reduction in the apical differentiated apoptosis-competent compartment. When FXR is activated in the intestine and in colon cancer cells, there is an induction of apoptosis and removal of genetically altered cells, which may otherwise progress to complete transformation. Thus, from a therapeutic standpoint, strategies aimed at reactivating FXR expression in colon tumors might be useful in treatment of colon cancer. [Cancer Res 2008;68(23):9589–94]

Introduction

The pathogenesis of colon cancer initially includes one or more genetically altered cells and requires many years to develop through a multistep process, which allows nutrients to modify the progression of the disease (1). Bile acids are cholesterol derivatives, necessary for the solubilization and absorption of lipids and lipid soluble vitamins in the gut (2). Studies in rodent models of intestinal cancer and human epidemiologic studies have linked elevated levels of bile acids to an increased incidence of colorectal cancer (3). Several pathways have been proposed to mediate the tumor promoting activity of bile acids in the postinitiation phase of intestinal tumorigenesis; however, the precise mechanism remains elusive. Bile acids are the natural ligands for the nuclear farnesoid X receptor (FXR, NR1H4; refs. 4, 5), a member of the nuclear hormone receptor family of transcription factors. FXR is highly expressed in the entero-hepatic system where it transcriptionally regulates bile acid and lipid metabolism. In the present study, we sought to investigate whether FXR plays a role in the progression of intestinal tumorigenesis. First, we show that FXR expression is restricted to the differentiated compartment of the intestinal mucosa and is low in intestinal tumors of both mice and humans. Second, we show that loss of FXR in two mouse models of intestinal tumorigenesis results in early mortality and increased tumor progression. Third, we provide evidence that the susceptibility of $FXR^{-/-}$ mice to intestinal tumorigenesis is unaffected by cholestyramine-mediated reduction in circulating bile acid levels, indicating that loss of FXR and not merely elevated bile acid concentrations increases susceptibility to tumorigenesis. Finally, using a xenograft model, we show that reactivation of FXR via adenoviral infection blocks tumor growth through the induction of proapoptotic pathways and repression of antiapoptotic as well as proinflammatory genes.

Materials and Methods

Mice. Pure strain C57BL/6J $FXR^{-/-}$ mice were kindly provided by Dr. D. Mangelsdorf (Southwestern Medical Center, Dallas, TX) and were generated by backcrossing with C57BL/6J mice for more than 15 generations the original $FXR^{-/-}$ mice [kindly provided by Dr. Frank Gonzalez (NIH, Bethesda, MD); ref. 6], which were in mixed strain background with C57BL/6J, sv129, FVBN. $FXR^{+/-}Apc^{Min/+}$ mice were generated by crossing $Apc^{Min/+}$ mice obtained from Jackson laboratory with $FXR^{-/-}$ mice, both on pure C57BL/6J background. Then, by intercrossing $FXR^{+/-}Apc^{Min/+}$, we generated $FXR^{-/-}Apc^{Min/+}$ mice. Nude mice for the xenograft experiments were obtained from the Jackson laboratory. Five million LS174T and 10 million HT29 colon cancer cells (American Type Culture Collection) were s.c. injected in the mice and tumor growth was measured with a 4-d repeated administration of adenoviruses. The Ethical Committee of the Consorzio Mario Negri Sud approved this experimental set-up.

Adenoviral constructs. VP16 and VP16FXR adenovirus (AdVP16 and AdVP16FXR) were generated using the Viral Power Adenoviral Expression System (Invitrogen). Briefly, to generate the VP16 adenovirus, the VP16 sequence (0.3 kb) from the pCMX-VP16 plasmid was subcloned into the pENTR4 shuttle vector using Sal I and XhoI restriction sites. Indeed, this shuttle vector containing VP16 was recombinated with the destination vector pAd/CMV/V5DEST. To generate the AdVP16FXR, the FXR sequence from the pCMX-VP16FXR (1.7 kb, kindly provided by Dr. D. Mangelsdorf) vector was subcloned into the pENTR4-VP16 shuttle vector using KpnI and BamHI restriction sites. Then, the pENTR4-VP16 and the pENTR4-VP16FXR

Note: Supplementary data for this article are available at Cancer Research Online (http://cancerres.aacrjournals.org/).

Requests for reprints: Antonio Moschetta, University of Bari and Consorzio Mario Negri Sud, Via Nazionale 8A, 66030 Santa Maria Imbaro (Chieti), Italy. Phone: 39-0872-570344; Fax: 39-0872-570299; E-mail: moschetta@negrisud.it.

doi:10.1158/0008-5472.CAN-08-1791

shuttle vectors were recombined with the destination vectors pAd/CMV/V5DEST. AdVP16 and AdVP16FXR were linearized with PacI restriction enzyme, and the digested products, after purification with Qiaex II gel extraction kit (Qiagen), were used to transfect 293A cells (Invitrogen) with Lipofectamine 2000 (Invitrogen) to generate the corresponding adenoviruses. The viruses were propagated into 293A cells. Crude viral lysate stocks were stored at −80°C until use.

Familial adenomatous polyposis patients. We obtained tissue (tumors and normal intestinal mucosa) samples from Dr. R. Valanzano (University of Florence, Florence, Italy) and Dr. R. Mariani-Costantini (University of Chieti-Pescara, Chieti, Italy). These unrelated familial adenomatous polyposis (FAP) patients were recruited for a previous study after approval by the Ethical Committee of the University "G. D'Annunzio" of Chieti. Written informed consent was obtained from each patient before mutation analysis and tissue harvesting. All the included cases presented with a classic FAP phenotype and harbored pathogenetic germline *APC* mutations.

Histology and immunohistochemistry. Tissue specimens were fixed in 10% formalin for 12 to 24 h, dehydrated, and paraffin embedded. Standard immunohistochemical procedures were performed. Briefly, 5-μm-thick sections were treated with 3% hydrogen peroxide for 5 min, to quench endogenous peroxidase, and subjected to antigen retrieval by boiling the slides in antigen unmasking solution (Vector-Laboratories, Inc.) for 15 min according to manufacturer's instructions. Sections were sequentially incubated for 60 min at room temperature in 50% nonimmune serum (from the host animal in which the secondary antibody was raised) in PBS (to avoid unspecific signal) and overnight at 4°C with the primary antibodies (rabbit polyclonal Ki67 from AbCam; FXR antibody was a generous gift from Phenex Pharmaceutical AG; rabbit polyclonal p21, C-19 from Santa Cruz; rat antimouse CD18 from BD Biosciences; human active β-catenin dephosphorylated on Ser37 and Thr41 from Upstate). Sections were washed 10 min in PBS and incubated for 30 min at room temperature with the secondary biotinylated antibody (Vector Laboratories). After several washing steps with PBS (3 washes, 5 min each), sections were incubated with the avidin-biotin complex (Vector Laboratories) for 30 min at room temperature. After washing in PBS, the peroxidase reaction was developed by incubation with 3,3′-diaminobenzidine (Sigma-Aldrich). Counterstaining was carried out with methylene-blue (Sigma-Aldrich). For negative controls, 1% nonimmune serum in PBS replaced the primary antibodies.

Aberrant crypt foci analysis. The aberrant crypt foci (ACF) detection and analysis was carried out as previously described (7). Briefly, after gross visual inspection, mouse colons were stored at −80°C until use. At the time of examination for ACF, colons were thawed in 2.5% formalin solution at room temperature, then fixed in 70% ethanol at 4°C for 30 min, and stained with 0.2% methylene blue for 2 min. Stained colons were transferred to 2.5% formalin solution at room temperature for up to 1 h and then examined in their entirety under a light microscope at ×40 or ×100 magnification, at which time the number and location of ACF were recorded.

Proliferation assay. LS174T were seeded at 1.5×10^4 cells per well in a 96-multiwell plate and infected with 100 multiplicity of infection (MOI) of AdVP16 or AdVP16FXR. After 48 h, cell proliferation was assayed by measuring DNA synthesis with the 5-bromo-2′-deoxy-uridine labeling and detection kit II (Roche) following the manufacturer's instructions. Postconfluence HT29 cells were treated with GW4064 (a gift from Dr. Ulrich Deuschle, Phenex Pharmaceuticals AG, Ludwigshafen, Germany) or vehicle in a 96-well plate at the indicated concentration for 48 h. Twelve hours before radioactivity quantification, 20 μL of 1 mCi [^{3}H] thymidine

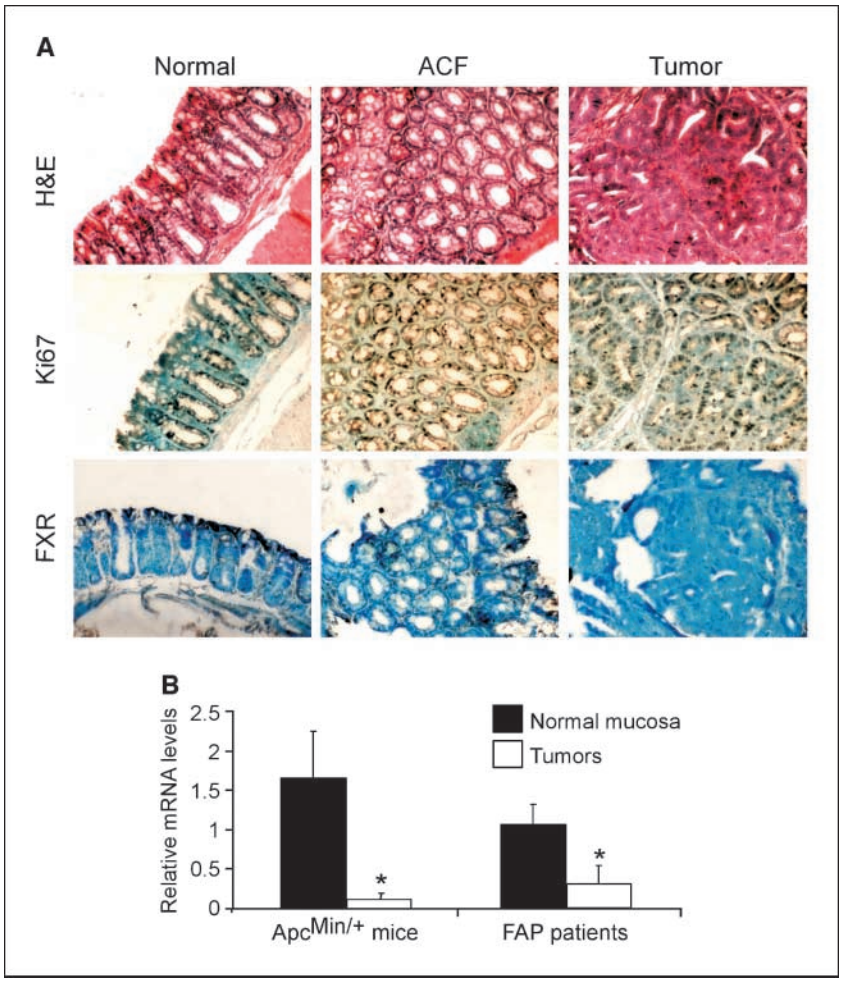

Figure 1. Down-regulation of FXR expression in mouse and human intestinal tumors. *A,* FXR expression is restricted to the apical surface of the colonic epithelia, while being absent in ACFs and adenomas of $Apc^{Min/+}$ mice. H&E and Ki67 staining was used for intestinal morphology and hyperproliferative zones, respectively. *B,* decreased mRNA levels of FXR were detected in tumors of $Apc^{Min/+}$ mice and FAP patients compared with the normal adjacent mucosa. *Columns,* mean of four independent determinations performed in duplicate; *bars,* SE. Cyclophilin was used as reference gene, and values were normalized to data obtained from normal intestinal mucosa.

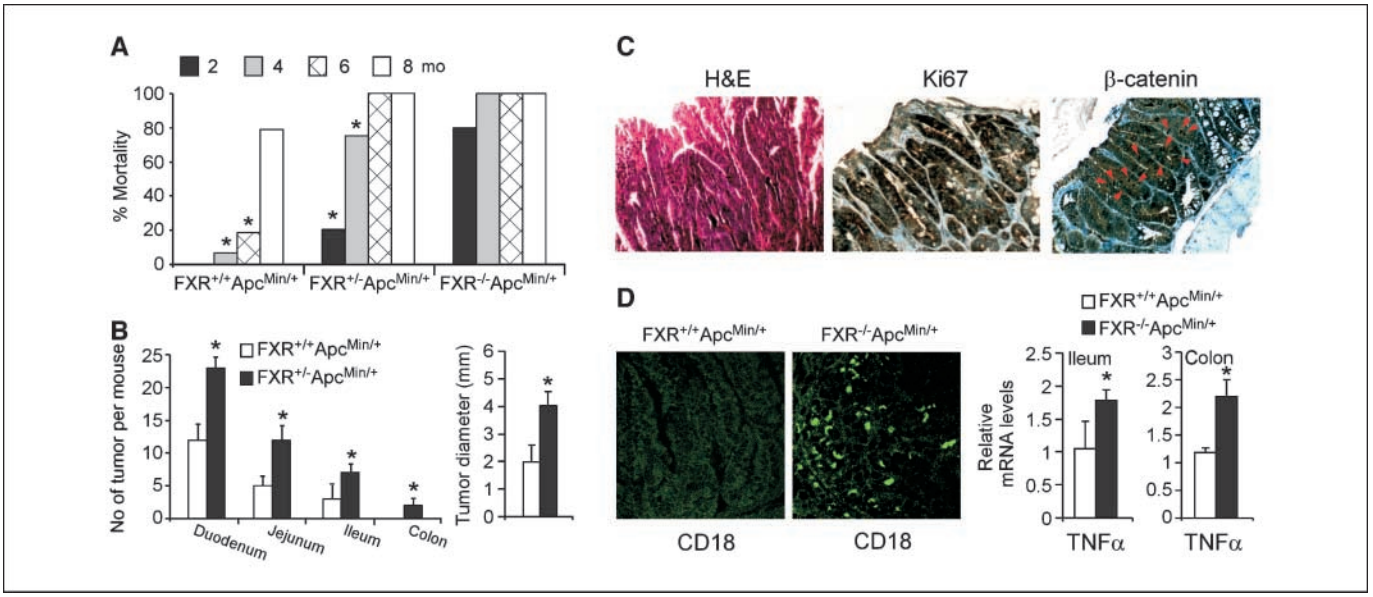

Figure 2. Loss of FXR increases susceptibility to intestinal tumorigenesis. *A,* whereas the majority of $FXR^{-/-}Apc^{Min/+}$ mice died at age 2 mo, around 30% of $FXR^{+/-}Apc^{Min/+}$ mice reached the age of 5 to 6 mo and allowed us to compare numbers and size of tumors versus $FXR^{+/+}Apc^{Min/+}$ mice. $Apc^{Min/+}$ mice in our colony survive up to maximum of 10 mo and start developing tumors at the age of 5 to 6 mo. Note that all the mice are in the same pure strain C57BL/6J background. *B,* surviving 4-mo-old $FXR^{+/-}Apc^{Min/+}$ mice presented a higher number of tumors compared with $FXR^{+/+}Apc^{Min/+}$ mice. Size of tumors observed in $FXR^{+/-}Apc^{Min/+}$ mice was larger than those of $FXR^{+/+}Apc^{Min/+}$ mice. *C,* upon histologic examination, the intestine of 7- to 8-wk-old $FXR^{-/-}Apc^{Min/+}$ mice contained numerous ACFs and large regions of severely disrupted crypt and villus units with loss of cytoarchitecture and adenoma-like lesions. These dysplastic regions presented an expansion of the basal, proliferative compartment (as shown by the Ki67 labeling) with accumulation of nuclear β-catenin in epithelial cells, and a concomitant reduction in the apical, differentiated compartment. *D,* massive infiltration of neutrophils and macrophages was observed in the intestinal mucosal dysplastic regions of $FXR^{-/-}Apc^{Min/+}$ mice by immunofluorence using an antibody against CD18 that recognizes the integrin β2 chain. Consequently, increased mRNA levels of proinflammatory TNFα were measured in the ileal and colonic mucosa of $FXR^{-/-}Apc^{Min/+}$ compared with $FXR^{+/+}Apc^{Min/+}$ mice. *Columns,* mean of four independent determinations performed in duplicate; *bars,* SE. Cyclophilin was used as reference gene, and values were normalized to data obtained in $FXR^{+/+}Apc^{Min/+}$ mice.*, $P < 0.05$.

were added to each well. To quantify the incorporation of [^{3}H] thymidine, the medium was removed and cells washed several times with PBS. After treatment with 5% (vol/vol) of trichloroacetic acid in PBS for 10 min at room temperature, DNA was solubilized with 200 μL of 0.1 mol/L NaOH containing 0.1% SDS (vol/vol). Then, radioactivity was quantified by liquid counting in a Beckman counter.

Apoptotic assay. LS174T were seeded at 6×10^5 cells per well in a 12-multiwell plate and infected with 100 MOI of AdVP16 or AdVP16FXR for 48 h. Then, apoptosis was investigated by determination of cytoplasmatic histone-associated DNA fragments using the cell death detection ELISA kit (Roche) following the manufacturer's instruction. Stainings for Annexin V-Alexa 568 (Roche) was carried out according to the manufacturer's protocols. Cells were finally washed with PBS and the coverslips mounted with MowiolTM (Calbiochem). For images examined at Zeiss LSM 510 confocal microscope (LSCM; ×1,260 magnification), optical sections were obtained with a ×63 oil immersion objective, at a definition of 1,024 × 1,024 pixels, with a pinhole diameter of 1 Airy unit for each emission channel. For terminal uridine deoxynucleotidyl transferase dUTP nick and labeling (TUNEL) assay *in vivo*, tissue specimens were fixed in 10% formalin for 12 to 24 h, dehydrated, and paraffin embedded. Detection of apoptosis at single-cell level based on labeling of DNA strand breaks was performed using the *In Situ* Cell Detection kit (Roche) following the manufacture instruction.

Real-time quantitative PCR. Real-time quantitative PCR (RTqPCR) primers were designed using Primer Express software. PCR assays were performed in 96-well optical reaction plates using the ABI 7500HT machine (Applied Biosystem). PCR assays were conducted in triplicate wells for each sample. Baseline values of amplification plots were set automatically, and threshold values were kept constant to obtain normalized cycle times and linear regression data. The reaction mixture per well used were as follows: 10 μL Power Syber Green (Applied Biosystem), 2.4 μL of primers at the final concentration of 150 nmol/L, 4.6 μL RNAase free water, and 3 μL cDNA (60 ng). For all experiments, PCR conditions used were as follows: denaturation at 95°C for 10 min, followed by 40 cycles at 95°C for 15 s, then at 60°C for 60 s. Quantitative normalization of cDNA in each sample was performed using cyclophilin as internal control. Relative quantification was performed using the $\Delta\Delta C_T$ method. Validated primers for RTqPCR are available upon request.

Statistical analysis. All results are expressed as mean ± SE. Data distribution and gene expression statistical analysis were performed using NCSS statistical and power analysis software 2007. Multiple groups were tested by one-way ANOVA or two-ways ANOVA repeated measures where appropriate, followed by Fisher's least significant difference test for unpaired data. Comparisons of two groups were performed using a Student's *t* test followed by Mann-Whitney *U* test where appropriate. A *P* value of <0.05 was considered significant.

Results and Discussion

In the normal intestine, we found that FXR expression is highest in the fully differentiated cells of the surface epithelium (Fig. 1*A*). To determine the role of FXR in transformed epithelium, we first examined the pattern of FXR expression in primary adenomas of mouse and human colon by immunohistochemistry and RTqPCR. FAP (8, 9) is a syndrome caused by mutations in the *APC* gene (10) and it is characterized by the early development of multiple polypoid tumors. In the mouse model of this disease (10), $Apc^{Min/+}$ mice develop tumors primarily in the small intestine and at later stages within the colon. Furthermore, in this model, tumors progress from precursor lesions, known as ACFs to polypoid adenomas. The expression of FXR was reduced in the ACFs and in the tumors of $Apc^{Min/+}$ mice (Fig. 1*B*). Similarly, compared with the normal adjacent mucosa, FXR expression was significantly

decreased in tumors of FAP patients (Fig. 1*B*). Thus, we conclude that FXR expression is low in mouse and human intestinal tumors compared with normal intestinal mucosa.

To understand if decreased FXR expression in tumors is simply a consequence of the lack of differentiation of transformed colonocytes, or if the loss of FXR contributes to tumor progression, we crossed pure strain C57BL/6J $FXR^{-/-}$ mice (6) with pure strain C57BL/6J $Apc^{Min/+}$ mice (10). Consistent with the latter, $FXR^{-/-}Apc^{Min/+}$ mice died at early age. Indeed, time of survival was directly proportional to the number of FXR alleles (Fig. 2*A*). The number and size of tumors were quantitated in 4- to 6-month-old mice. A significant increase was seen in the number and size of tumors of $FXR^{+/-}Apc^{Min/+}$ mice relative to $FXR^{+/+}Apc^{Min/+}$ mice (Supplementary Fig. S1; Fig. 2*B*). Because $FXR^{-/-}Apc^{Min/+}$ mice die before the age of 3 months, they were not included in this tumor count. Nevertheless, upon macroscopic examination, the intestine of 7- to 8-week-old $FXR^{-/-}Apc^{Min/+}$ mice already contained numerous ACF and large regions of severely disrupted crypt and villus units with loss of cytoarchitecture and adenoma-like lesions (Fig. 2*C*; ref. 11). Upon histologic examination, these dysplastic regions presented an expansion of the basal, proliferative compartment (11) both in the ileum and in the colon, and a concomitant reduction in the apical, differentiated compartment (Fig. 2*C*). It is known that mice lacking FXR have a compromised intestinal epithelial barrier with increased ileal levels of bacteria and numbers of neutrophils per villus (12). Here, we found massive neutrophils and macrophages infiltration via CD18 labeling in the mucosa of $FXR^{-/-}Apc^{Min/+}$ mice with increased nuclear β-catenin accumulated and Ki67-positive epithelial cells (Fig. 2*C* and *D*). Activated macrophages are able to further promote Wnt/β-catenin signaling and tumor development in the intestinal mucosa of $Apc^{Min/+}$ mice through tumor necrosis factor-α (TNFα; ref. 13), and TNFα blocking has been shown to reduce intestinal tumors in the azoxymethane (AOM)-dextran sulfate sodium (DSS) mouse model of colon carcinogenesis associated with chronic colitis (14). Thus, we measured mRNA levels of TNFα and found a significant increase in expression in the ileum and colon of $FXR^{-/-}Apc^{Min/+}$ mice compared with $FXR^{+/+}Apc^{Min/+}$ mice (Fig. 2*D*). Consequently, we also tested the role of FXR in the AOM-DSS mouse model of intestinal tumorigenesis (14). As in the $Apc^{Min/+}$ model, the absence of FXR mice resulted in increased susceptibility to intestinal tumorigenic early events as shown by the increased number and size of colonic dysplastic areas per mouse compared with $FXR^{+/+}$ mice (Supplementary Fig. S2; Fig. 3*A*). Furthermore, $FXR^{-/-}$ mice showed higher sensitivity to the treatment regimen as shown by an increase in mortality (Fig. 3*A*). From these results, we conclude that loss of FXR in two mouse models of intestinal tumorigenesis results in early mortality and tumor progression. Although the precise mechanism by which the loss of FXR results in increased tumor susceptibility is not completely clear, our data indicate that the promotion of Wnt signaling caused by increased TNFα production and mucosal infiltration of activated neutrophils and macrophages may play a contributing role.

$FXR^{-/-}$ mice have an increased bile acid pool size due to increased hepatic bile acid synthesis (6, 15). It has been suggested that bile acids contribute to hepatocellular carcinogenesis observed in the $FXR^{-/-}$ mice (16, 17). Similarly, the high susceptibility of $FXR^{-/-}$ mice to intestinal tumorigenesis might relate to the elevated bile acid levels per se rather than a direct effect of the loss of FXR in the intestine. To this end, we performed two experiments with a diet containing 2% of the bile acid binding resin cholestyramine, which is able to significantly reduce the circulating

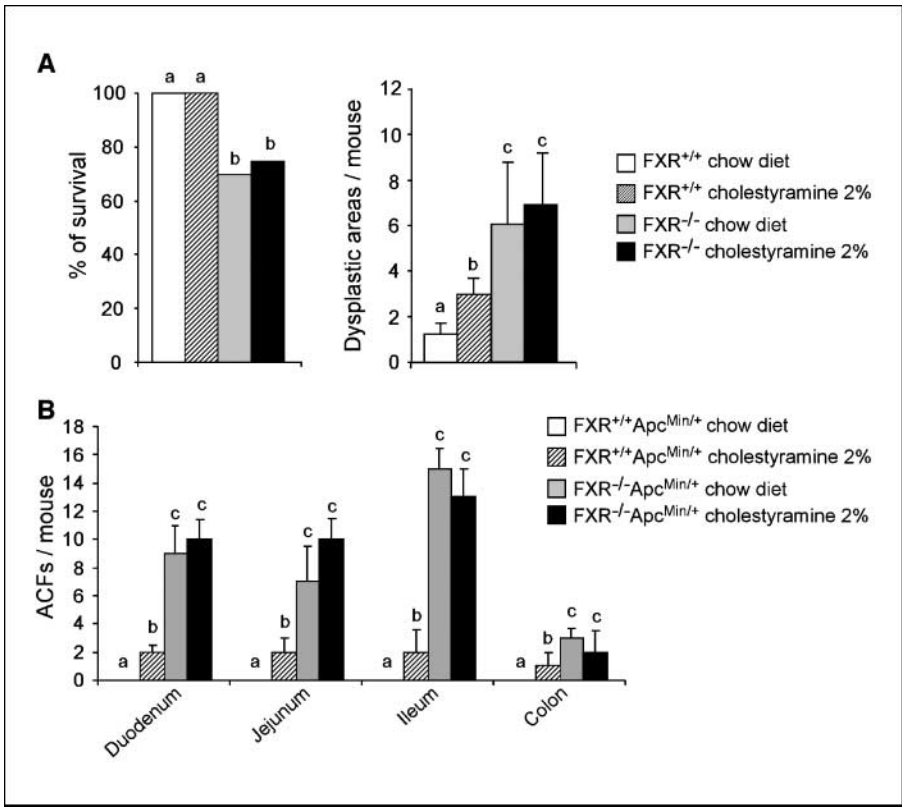

Figure 3. Susceptibility of $FXR^{-/-}$ mice to intestinal tumorigenesis is unaffected by cholestyramine-mediated reduction in circulating bile acid levels. *A,* the AOM-DSS model of colon carcinogenesis (14) was used under different dietary regimens in both $FXR^{+/+}$ and $FXR^{-/-}$ mice. The protocol resulted in early mortality for $FXR^{-/-}$ mice. Compared with chow diet regimen, cholestyramine treatment significantly increased the number of dysplastic lesions in the $FXR^{+/+}$ mice, although it did not affect the susceptibility to intestinal tumorigenesis of $FXR^{-/-}$ mice. *B,* $FXR^{+/+}Apc^{Min/+}$ and $FXR^{-/-}Apc^{Min/+}$ mice of age 1 mo were treated with cholestyramine for 4 wk. There was no significant difference in the number of ACFs in the four intestinal segments (duodenum, jejunum, ileum, and colon) of the $FXR^{-/-}Apc^{Min/+}$ mice treated with cholestyramine-containing diet versus chow diet. Interestingly, although no ACFs were detected in the intestine of 2-mo-old $Apc^{Min/+}$ mice on chow diet, few ACFs appeared in the four segments of the intestine of the $Apc^{Min/+}$ mice of the same age treated with cholestyramine. Different lower case letters indicate statistical significance ($P < 0.05$).

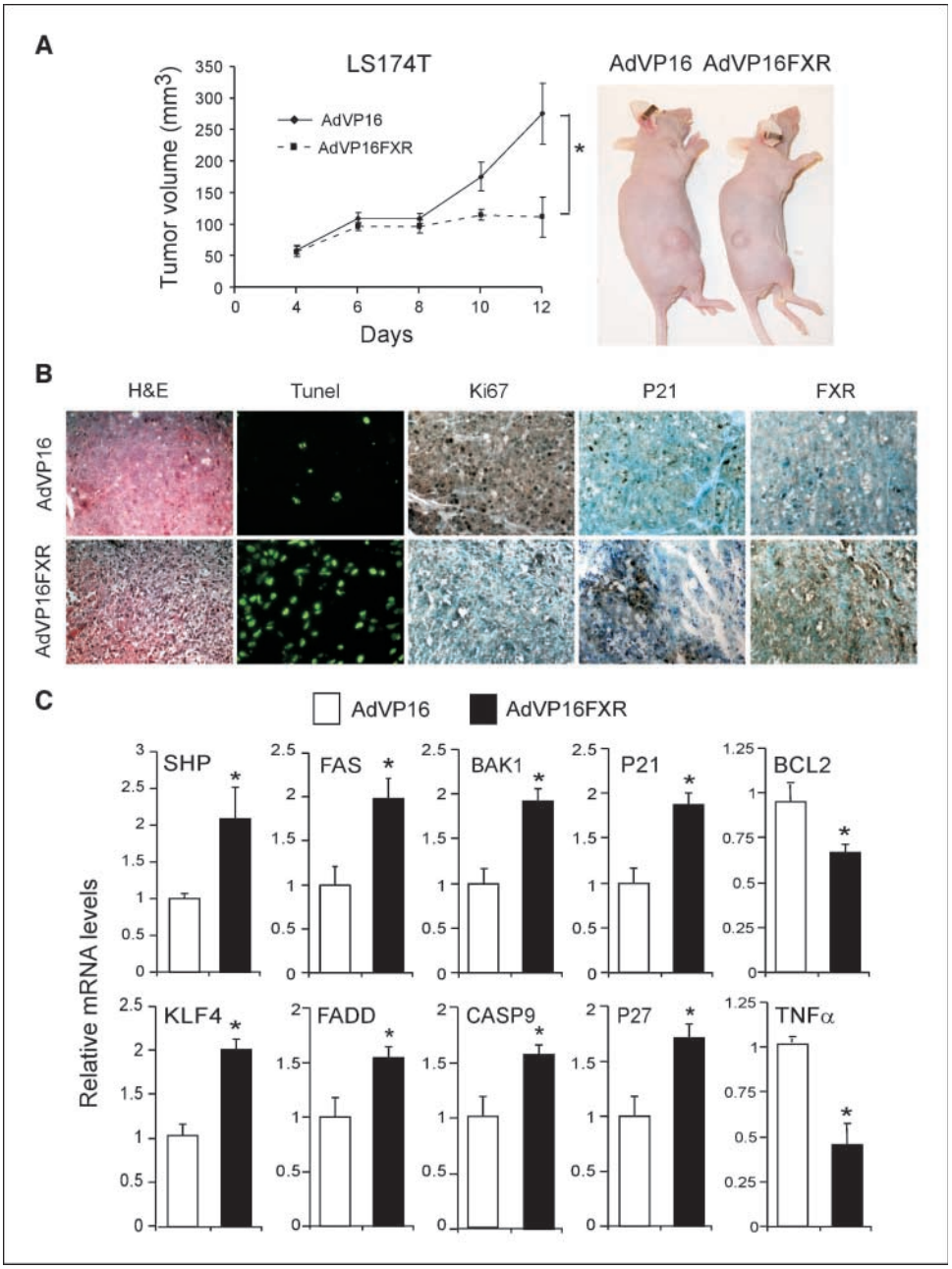

Figure 4. Reactivation of FXR in colon cancer cells via adenoviral infection blocks tumor growth through the induction of proapoptotic pathways. *A,* AdVP16FXR intratumoral administration reduced tumor growth in the nude mice with s.c. injection of LS174T cells with respect to AdVP16. *B,* H&E, TUNEL, Ki67, P21, and FXR staining of the tumors revealed a net activation of apoptotic events with reduction in Ki67 labeling after administration of AdVP16FXR. *C,* when LS174T cells were infected with AdVP16FXR, significant increased mRNA levels of FXR target gene *SHP* were paralleled by an increase in the mRNA levels of a proapoptotic network of genes (*FAS, BAK1, P21, KLF4, FADD, CASP9*, and *P27*) and a decrease in mRNA levels of antiapoptotic *BCL2* and proinflammatory *TNFα* genes. *Columns,* mean of four independent determinations performed in duplicate; *bars,* SE. Cyclophilin was used as reference gene and values were normalized to data obtained from AdVP16 infection. *, $P < 0.05$.

bile acid levels (18). First, we treated 1-month-old male $FXR^{+/+}Apc^{Min/+}$ and $FXR^{-/-}Apc^{Min/+}$ mice with cholestyramine for 4 weeks. We found no significant difference in the number of ACFs in the four intestinal segments (duodenum, jejunum, ileum, and colon) of the $FXR^{-/-}Apc^{Min/+}$ mice treated with cholestyramine-containing diet versus chow diet (Fig. 3*B*). Interestingly, although no ACFs were detected in the intestine of 2-month-old $Apc^{Min/+}$ mice on chow diet, few ACFs appeared in the 4 segments of the intestine of the $Apc^{Min/+}$ mice of the same age treated with cholestyramine. Second, we used the AOM-DSS model to confirm the data obtained in the genetic model. Also in this model, compared with chow diet regimen, cholestyramine did not affect the susceptibility to intestinal tumorigenesis of $FXR^{-/-}$ mice (Supplementary Fig. S2; Fig. 3*A*). These data suggest that, unlike the liver, the absence of FXR from the intestinal epithelium and not merely elevated bile acid concentrations per se increases susceptibility to tumorigenesis.

Although these studies clearly established a connection between the loss of FXR and intestinal tumorigenesis, we sought to gain additional mechanistic insight and determine if and how FXR activation might protect against intestinal tumorigenesis using gain-of-function studies. VP16 is a strong transcriptional activator, and when expressed as a chimeric protein, VP16FXR results in the constitutive induction of FXR target genes. Our goal was to determine if reactivation of FXR in intestinal cancer cells was able to block tumor growth using a xenograft mouse model. To this end, we generated adenoviruses expressing the VP16 and VP16FXR chimeras. We injected LS174T colon cancer cells (11) s.c. in nude mice and followed tumor growth after administration of AdVP16 or AdVP16FXR. Activated FXR markedly increased apoptosis, as

shown by TUNEL assay (Fig. 4*B*), reduced proliferation, as shown by the Ki67 labeling (Fig. 4*B*), and significantly blocked tumor growth (Fig. 4*A*). These results were confirmed in the xenograft model using a second colon cancer cell line (HT29; Supplementary Fig. S3). In line with this finding, FXR activation has been shown to regulate apoptosis also in the vasculature (19) and in breast cancer (20). Compared with AdVP16, AdVP16FXR infection in LS174T cells induced an increase in apoptotic events, as shown by Annexin V labeling and nucleosome enrichment, paralleled by a decrease in BrdUrd incorporation (Supplementary Fig. S4*A*). In addition, the synthetic FXR ligand GW4064 was also able to activate apoptosis both in the cellular model (Supplementary Fig. S4*B*) and in the normal intestinal mucosa *in vivo* (Supplementary Fig. S5). An intriguing scenario arises when we started searching for the FXR-driven transcriptome to explain the observed phenotype. A significant increase in mRNA levels of proapoptotic genes (Fig. 4*C*) were observed in AdVP16FXR versus AdVP16 infected LS174T cells. At the same time, there was a significant decrease in mRNA levels of antiapoptotic *BCL2* and proinflammatory *TNFα* genes, whereas no differences were observed in the mRNA levels of genes targeted by the nuclear β-catenin-TCF complexes (11). Expression levels of the known FXR target gene *small heterodimer partner* (*SHP*) are reported as control. These data show that activation of FXR seems to block tumor growth and to induce in normal and transformed enterocytes a network of proapoptotic genes that are down-regulated in tumors (Supplementary Fig. S6) and are known to play key roles in cancer prevention.

In summary, our data suggest that it is unlikely that the tumor-promoting activity of bile acids occurs as a function of their ability to activate FXR in the intestine. However, FXR activity is relevant to the pathogenesis of intestinal cancer. Our gain- and loss-of-function studies support the hypothesis that FXR suppresses intestinal tumorigenesis. When FXR is absent, there is a promotion of Wnt signaling via increased infiltrating neutrophils and TNFα production with expansion of the basal proliferative compartment both in the ileum and in the colon, and a concomitant reduction in the apical, differentiated apoptosis-competent compartment. This scenario leads to increased tumor progression and early mortality in mice. On the other hand, when FXR is activated in the differentiated normal enterocytes and in colon cancer cells, there is an induction of apoptosis and removal of genetically altered cells, which may otherwise progress to complete transformation. Thus, from a therapeutic standpoint, strategies aimed at reactivating FXR expression in colon tumors might be useful in the treatment of colon cancer.

Disclosure of Potential Conflicts of Interest

No potential conflicts of interest were disclosed.

Acknowledgments

Received 5/12/2008; revised 9/10/2008; accepted 10/2/2008.

Grant support: Start Up Grant 2005 of the Italian Association for Cancer Research (Associazione Italiana per la Ricerca sul Cancro, Milan), the University of Bari (Bari, Italy), and by the NIH grant CA114109-02. S. Murzilli is supported by a fellowship from Cassa di Risparmio della Provincia dell'Aquila. D.R. Schmidt is supported by the NIH Pharmacological Sciences Training Grant (GM007062) and the Medical Scientist Training Program.

The costs of publication of this article were defrayed in part by the payment of page charges. This article must therefore be hereby marked *advertisement* in accordance with 18 U.S.C. Section 1734 solely to indicate this fact.

We thank H. Clevers, U. Deuschle, V. Evangelista, S. Kliewer, D. Mangelsdorf, R. Mariani-Costantini, G. Palasciano, A. Poggi, P. Portincasa, C. Rossi, C. Simone, R. Valanzano for invaluable tools, help, and discussion, and G. Losasso, M. Petruzzelli, and all members from the laboratory for criticisms and assistance during this study.

References

1. Kinzler KW, Vogelstein B. Lessons from hereditary colorectal cancer. Cell 1996;87:159–70.
2. Hofmann AF. The continuing importance of bile acids in liver and intestinal disease. Arch Intern Med 1999;159:2647–58.
3. Lipkin M, Reddy B, Newmark H, Lamprecht SA. Dietary factors in human colorectal cancer. Annu Rev Nutr 1999;19:545–86.
4. Makishima M, Okamoto AY, Repa JJ, et al. Identification of a nuclear receptor for bile acids. Science 1999;284:1362–5.
5. Parks DJ, Blanchard SG, Bledsoe RK, et al. Bile acids: natural ligands for an orphan nuclear receptor. Science 1999;284:1365–8.
6. Sinal CJ, Tohkin M, Miyata M, Ward JM, Lambert G, Gonzalez FJ. Targeted disruption of the nuclear receptor FXR/BAR impairs bile acid and lipid homeostasis. Cell 2000;102:731–44.
7. Myung SJ, Rerko RM, Yan M, et al. 15-Hydroxyprostaglandin dehydrogenase is an *in vivo* suppressor of colon tumorigenesis. Proc Natl Acad Sci U S A 2006;103:12098–102.
8. Kinzler KW, Nilbert MC, Su LK, et al. Identification of FAP locus genes from chromosome 5q21. Science 1991;253:661–5.
9. Powell SM, Petersen GM, Krush AJ, et al. Molecular diagnosis of familial adenomatous polyposis. N Engl J Med 1993;329:1982–7.
10. Su LK, Kinzler KW, Vogelstein B, et al. Multiple intestinal neoplasia caused by a mutation in the murine homolog of the APC gene. Science 1992;256:668–70.
11. Van de Wetering M, Sancho E, Verweij C, et al. The β-catenin/TCF-4 complex imposes a crypt progenitor phenotype on colorectal cancer cells. Cell 2002;111:241–50.
12. Inagaki T, Moschetta A, Lee YK, et al. Regulation of antibacterial defense in the small intestine by the nuclear bile acid receptor. Proc Natl Acad Sci U S A 2006;103:3920–5.
13. Oguma K, Oshima H, Aoki M, et al. Activated macrophages promote Wnt signalling through tumour necrosis factor-α in gastric tumour cells. EMBO J 2008;27:1671–81.
14. Popivanova BK, Kitamura K, Wu Y, et al. Blocking TNF-α in mice reduces colorectal carcinogenesis associated with chronic colitis. J Clin Invest 2008;118:560–70.
15. Kok T, Hulzebos CV, Wolters H, et al. Enterohepatic circulation of bile salts in farnesoid X receptor-deficient mice: efficient intestinal bile salt absorption in the absence of ileal bile acid-binding protein. J Biol Chem 2003;278:41930–7.
16. Yang F, Huang X, Yi T, Yen Y, Moore DD, Huang W. Spontaneous development of liver tumors in the absence of the bile acid receptor farnesoid X receptor. Cancer Res 2007;67:863–7.
17. Kim I, Morimura K, Shah Y, Yang Q, Ward JM, Gonzalez FJ. Spontaneous hepatocarcinogenesis in farnesoid X receptor-null mice. Carcinogenesis 2007;28:940–6.
18. Huang W, Ma K, Zhang J, et al. Nuclear receptor-dependent bile acid signaling is required for normal liver regeneration. Science 2006;312:233–6.
19. Bishop-Bailey D, Walsh DT, Warner TD. Expression and activation of the farnesoid X receptor in the vasculature. Proc Natl Acad Sci U S A 2004;101:3668–73.
20. Swales KE, Korbonits M, Carpenter R, Walsh DT, Warner TD, Bishop-Bailey D. The farnesoid X receptor is expressed in breast cancer and regulates apoptosis and aromatase expression. Cancer Res 2006;66:10120–6.

Nuclear Bile Acid Receptor FXR Protects against Intestinal Tumorigenesis

Salvatore Modica, Stefania Murzilli, Lorena Salvatore, et al.

Cancer Res 2008;68:9589-9594.